Chimia 54 (2000) 593–601

ISSN 0009–4293

Molecular-Based Magnetism in High-Spin Molecular Clusters and Three-Dimensional Networks Based on Cyanometalate Building Blocks

Melanie Pilkington* and Silvio Decurtins

Abstract: The field of molecule-based magnets is a relatively new branch of chemistry, which involves the design and study of molecular compounds that exhibit a spontaneous magnetic ordering below a critical temperature, T_c. One major goal involves the design of materials with tuneable Tc's for specific applications in memory storage devices. Molecule-based magnets with high magnetic ordering temperatures have recently been obtained from bimetallic and mixed-valence transition metal μ-cyanide complexes of the Prussian blue family. Since the μ-cyanide linkages permit an interaction between paramagnetic metal ions, cyanometalate building blocks have found useful applications in the field of molecule-based magnets. Our work involves the use of octacyanometalate building blocks for the self-assembly of two new classes of magnetic materials namely, high-spin molecular clusters which exhibit both ferromagnetic intra- and intercluster coupling, and specific extended network topologies which show long-range ferromagnetic ordering.

Keywords: Cyanometalates · Extended networks · High-spin molecules · Molecule-based magnets · Molecular clusters · Supramolecular chemistry

1. Introduction

As the limits of silicon are approached, the possibility of 'engineering up' from a molecule to functioning electronic devices offers one alternative route to the design of materials for use on the molecular scale and beyond. The aim is to design and assemble molecular devices that will reduce dimensions and increase speed by orders of magnitude. Chemists are thus targeting molecular systems that are easily switchable between two available states. In this respect, molecular magnetism is a rapidly developing field [1] since in general, nanomagnetic materials easily reverse their magnetic moments in a magnetic field and are already widely used in information storage.

Molecular magnetism can be considered to be supramolecular in its nature, since it results from the collective features of components bearing free spins and on their arrangement in organised assemblies [2]. The engineering of molecular magnetic systems thus requires the search for paramagnetic metal ions and their arrangement in suitable supramolecular architectures so as to induce spin coupling and alignment. One of the main challenges is the design of molecule-based compounds exhibiting spontaneous magnetisation with high critical temperature T_c values, since most memory devices are expected to work at or around room temperature [3]. In the majority of cases these compounds contain two kinds of spin carriers, either two different metal ions, or a metal ion and an organic radical. Current research in this field aims not only to improve the magnetic properties, but also to achieve unusual properties, which to date have not yet been realised in conventional magnets.

2. Crystal Engineering

One of the challenges for a chemist in the field of molecular magnets is to control molecular topology in order to obtain interactions between spin carriers in three dimensions. To build a three-dimensional network, a specific type of building block is necessary. Cleverly designed building blocks provide a molecular-scale 'legokit' which enables chemists to design and engineer novel materials having a predictable structural order, as well

*Correspondence: Dr. M. Pilkington
Departement für Chemie und Biochemie
Universität Bern
Freiestrasse 3
CH-3012 Bern
Tel.: +41 31 631 42 96
Fax: +41 31 631 39 93
E-Mail: melanie.pilkington@iac.unibe.ch

as a useful set of solid-state properties. In earlier work we have shown that it is possible to develop a strategy for the self-assembly of supramolecular systems based on transition-metal oxalates, which typically behave as host/guest compounds with different lattice dimensionalities [4][5]. Our approach involves the build up of three-dimensional frameworks under mild chemical conditions using building blocks specially chosen to achieve the desired bonding networks connecting the spin-bearing species [4]. More recently, we have begun to apply this concept to include cyanometalates which are distant cousins of the Prussian blue family of molecules.

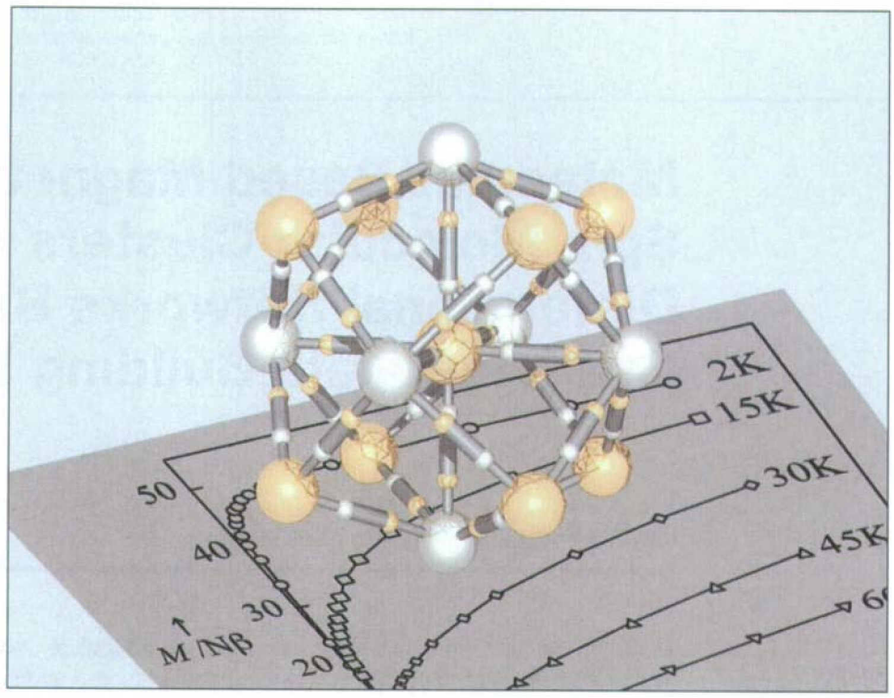

Fig. 1. Representation of the $[Mn^{II}_9(\mu\text{-}CN)_{30}\text{-}Mo^{V}_6]$ cluster core, superimposed over the field dependence of magnetisation. The gold spheres represent Mn^{II} ions and the silver spheres represent Mo^{V} ions and the bonds between them represent μ-cyano ligands. The saturation value of the magnetisation occurs near the expected $M_S/N\beta$ value of 51 which indicates that this molecule currently holds the world record for the largest $S = {}^{51}/_{2}$ ground state spin value.

3. The Prussian Blues

Prussian blue is one of the oldest co-ordination compounds reported in the chemical literature [6] and its synthesis actually precedes Werner's concept of coordination chemistry by almost 200 years [7]. Its name is derived from its intense colour, since mixing together an aqueous pale yellow solution of $K_4[Fe(CN)_6]$ with a light orange solution of an iron(III) salt immediately results in a deep blue precipitate of a mixed-valent cyanoferrate of stoichiometry $Fe^{III}_4[Fe^{II}(CN)_6]_3 \cdot 15H_2O$. Substitution of iron(III) and iron(II) by other ions A and B leads to a series of compounds whose structural topology is face-centred cubic, closely resembling that of simple rock salt. When paramagnetic metal ions are used, compounds with a range of magnetic properties have been reported since the linear -A-N≡C-B- sequence permits an interaction between paramagnetic metal ions. The need for higher ordering temperatures has provided the driving force for several research teams to probe, in detail, the nature of the -A-N≡C-B- interactions. In 1995, Verdaguer and co-workers were able to increase the Curie temperature and overcome the room-temperature barrier with a Prussian blue-like $Cr^{III}/[V^{II}\text{-}V^{III}]$ compound which orders at T_c = 315 K [8]. With this first discovery of a room-temperature molecular-based magnet, there is currently a revival in Prussian blue chemistry [9].

New families of compounds related to Prussian blue which contain paramagnetic centres are particularly attractive candidates for new molecular magnets since, as well as promoting the formation of strong magnetic interactions between adjacent spin centres, the synthesis of the bimetallic systems is flexible. The self-assembly process involves the reaction of stable cyanometalates $[B(CN)n]^{k-}$ with metallic cations A^{l+}, where A and B are transition- metal ions with various oxidation states. By carefully selecting the appropriate cyanometalate building blocks together with a metallic cation, it should be possible to assemble a specific structural topology which, to a certain extent reflects the preferred co-ordination geometry of the metal ions concerned. Nature then provides a wide range of metals with different spin and oxidation states, which can be incorporated into the resulting structures. These features give us considerable control over the structure of the solid and allow us to tune the magnitude of the local magnetic exchange interactions as well as alter the physical properties of the compounds.

In this respect, we are currently exploring the use of the octacyanometalate precursor $[B(CN)_8]^{n-}$, where B = Mo^{IV}, Mo^{V}, W^{IV}, W^{V} and Nb^{IV}, for the self-assembly of two new series of supramolecular coordination compounds. The first falls into the class of high-spin molecular clusters [10] and the second are three-dimensionally linked supramolecular assemblies [11]. We report herein our present findings with regards to the synthesis, structure determination and physical properties of these new coordination solids.

4. High-Spin Molecular Clusters

The study of molecules possessing unusually large spin (S) values in their ground state is an area of intense current research in particular, since it has become apparent that a relatively large ground state S value is one of the necessary requirements for molecules to be able to exhibit the new phenomenon of single-molecule magnetism [12]. One area in which high-spin molecules are often encountered is in cluster chemistry. The synthesis and investigation of the magnetic properties of large molecular clusters incorporating transition-metal ions is thus one of the current challenges in molecular magnetism [13][14]. High-spin clusters with $S > 10$ are still however very rare, until very recently [10][21], the highest value reported was $S = {}^{33}/_{2}$ for a co-crystallised Fe_{17} and Fe_{19} species. The most accurately investigated system so far belongs to the series of manganese carboxylates of general formula $[Mn_{12}O_{12}(RCOO)_{16}]$ with a varying number of

water molecules [15]. For this cluster, a slow relaxation of the magnetisation was detected at low temperature, similar to the blocking temperature of superparamagnets [16]. Consequently, in the low-temperature regime, this cluster behaves like a single-molecule magnet, showing also molecular hysteresis effects.

4.1. *Structural Topology*

By exploiting the coordination chemistry of the octacyanomolybdenate building block $[Mo^{V}(CN)_8]^{3-}$ with various M^{2+} metal ions, we have obtained a new class of compounds, which is structurally very different from the Prussian blue phases. Reaction of a 3:2 molar ratio of $[Mn^{II}(H_2O)_6](NO_3)_2{\cdot}xH_2O$ and $(NBu_4)_3[Mo^{V}(CN)_8]$ in methanol: propanol 1:1 yielded large and well-shaped single crystals whose magnetic properties were unusual and extremely interesting. The single crystal X-ray analysis at 223 K revealed that the compound is a cyano-bridged molecular cluster, **1** [10]. The cluster of formula $[Mn^{II}\{Mn^{II}(MeOH)_3\}_8(\mu\text{-}CN)_{30}\{Mo^{V}(CN)_3\}_6]{\cdot}5\ MeOH{\cdot}2H_2O$ (**1**) is comprised of fifteen cyano-bridged metal ions, namely nine Mn^{II} ions ($S = {}^5/_2$) and six Mo^{V} ions ($S = {}^1/_2$), giving a total of 51 unpaired electrons. For simplification, the molecular configuration of an idealised pentadecanuclear cluster core with O_h symmetry is sketched in Fig. 1. The nine Mn^{II} ions define a body-centred cube, and the six Mo^{V} ions constitute an octahedron. The Mo^{V}-CN-Mn^{II} geometry is such that the atoms are all linked to form an aesthetically pleasing topological pattern in which the polyhedron spanned by the peripheral metal ions is closest in geometry to a rhombic dodecahedron. Fig. 2 shows an ORTEP plot of the molecule. The compound crystallises in a monoclinic space group ($C2/c$) and the cluster itself has a C_2 point-group symmetry with the central Mn^{II} ion lying on the crystallographic two-fold axis. Additional ligands fill the coordination sphere of the peripheral metal ions, and complete the charge balance to give a neutral cluster. Three methanol molecules are ligated to the outer Mn^{II} ions, which increases their coordination number to six. Analogously, three terminal cyano ligands coordinate to each Mo^{V} ion, establishing an eight-fold coordination and giving the overall $[Mo^{V}(CN)_8]^{3-}$ stoichiometry.

The spin-bearing centres in the cluster (with the exception of the central Mn^{II} ion) are all located at the periphery of the molecule and are essentially free from

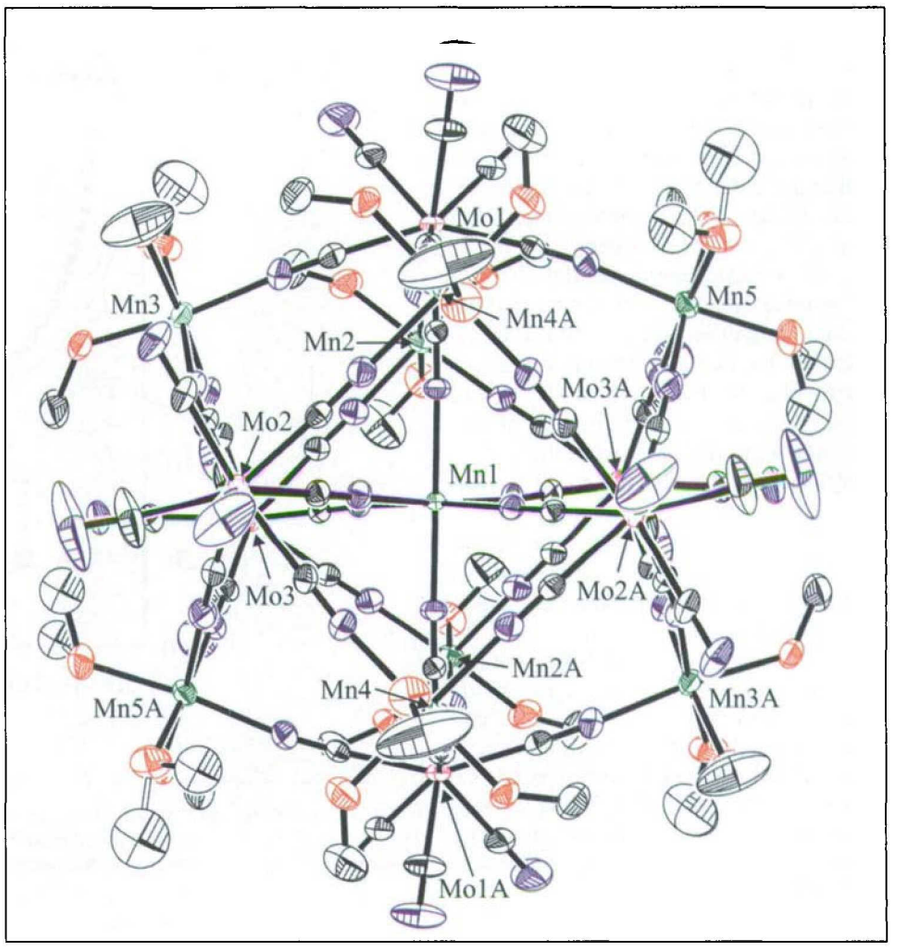

Fig. 2. ORTEP representation of the molecular structure of $[Mn^{II}\{Mn^{II}(MeOH)_3\}_8(\mu\text{-}CN)_{30}\{Mo^{V}CN)_3\}_6]$ (1); for clarity only the Mn^{II} and Mo^{V} atoms are labelled and the H-atoms are omitted.

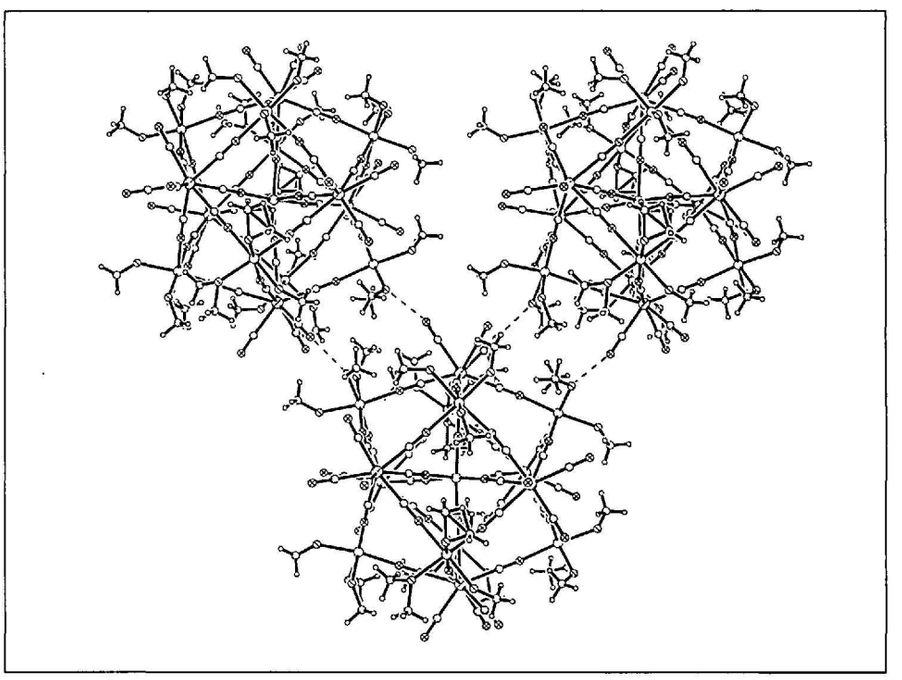

Fig. 3. A plot of three nearest neighbour cluster molecules (**1**) showing the close edge contacts between the Mn^{II} and the Mo^{V} ions. The dotted lines represent the H-bonding interactions O–H···N.

any shielding by bulky organic ligands. Two types of geometry for the Mo–C–N–Mn bridges are found in the title compound. Those which involve the central Mn^{II} ion are fairly linear, whereas the peripheral Mo–C–N–Mn bridges are essentially linear at the cyanide carbon, but bent at the cyanide nitrogen.

An extended intermolecular H-bonded network connects each cluster to eight nearest neighbours. Fig. 3 shows the H-bonding interactions between three nearest neighbour cluster molecules. All of these O–H···N contacts are well within the sum of the van der Waals radii (2.9 Å), indicative of 'medium strength' H-bonds. This extended intercluster H-bonded network, where the MeOH donors and CN acceptors are connected in a regular donor-acceptor sequence to give a continuous three-dimensional array, results in close nearest neighbour contacts between metal ions at the edges of the clusters [Mo···Mn (6.97 to 7.58 Å) and Mn···Mn (7.20 to 7.58 Å)]. All remaining cyanide and methanol molecules not involved in intercluster H-bonding interactions form H-bonds with neighbouring solvent molecules. The solvent molecules (MeOH and H_2O) occupy channels between the clusters, filling up the remaining unoccupied space in the crystal lattice.

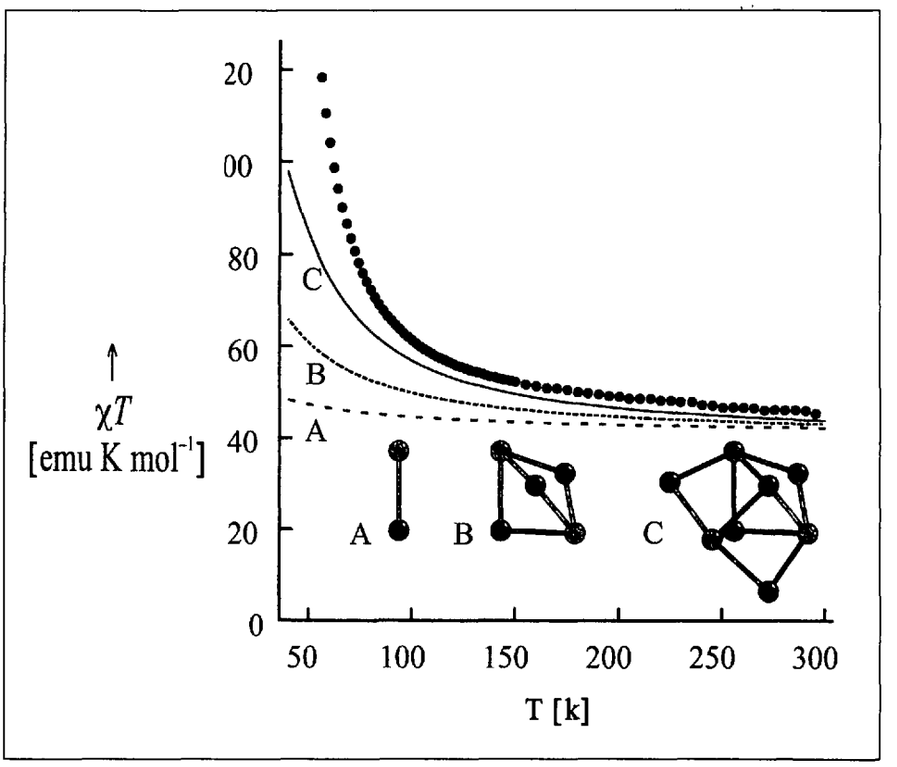

Fig. 4. Temperature dependence of $\chi_M T$ above 50 K for the polycrystalline cluster compound **1**. The lines A, B, C represent calculated results for the corresponding cluster fractions (Mn^{II}: dark spheres; Mo^{V}: light spheres) using the exchange parameter, J = 7 cm^{-1}.

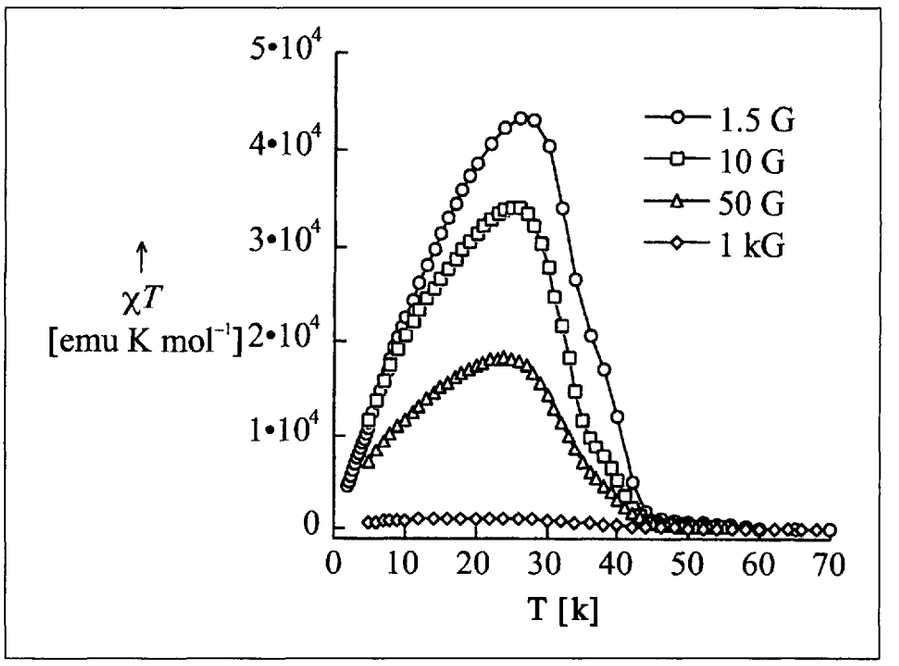

Fig. 5. Temperature dependence of $\chi_M T$ for the polycrystalline cluster compound **1** at different field values.

4.2. *Magnetic Properties*

Having synthesised and structurally characterised a molecular compound possessing 51 unpaired electrons, the investigation of the magnetic behaviour became of prime interest. The magnetic properties in the high temperature regime, above 50 K are characterised by ferromagnetic intracluster coupling [10]. Fig. 4 shows the corresponding plot of $\chi_M T$ *vs* T demonstrating a gradual increase of $\chi_M T$ with the lowering of temperature. Even at 300 K, the experimental value of $\chi_M T$ = 46 emu·K·mol^{-1} is slightly higher than the calculated spin-only value of $\chi_M T$ = 40.9 emu·K·mol^{-1} for a cluster comprising of nine non-interacting Mn^{II} (g = 2.0, S = $^5/_2$) and six non-interacting Mo^{V} (g = 1.98, S = $^1/_2$) centres, demonstrating the effect of the ferromagnetic intracluster exchange.

A competitive interplay of intra- and intercluster interactions leads to a very interesting magnetic regime in the temperature range below 50 K. Fig. 5 shows the corresponding plot of $\chi_M T$ *vs* T for different values of the applied field. Most significantly, the gradual increase of $\chi_M T$ with the lowering of temperature shows a clear break around 44 K, where $\chi_M T$ starts to rise steeply reaching 4·10^4 emu·K·mol^{-1} for an applied field of 1.5 G. This abrupt increase of $\chi_M T$ indicates the onset of cooperative ferromagnetic intercluster interactions. This relatively high onset of intercluster correlations can be due to both exchange and magnetic dipole-dipole interactions [17]. The former are facilitated by sixteen hydrogen bonds per cluster of the type N···H–O which are present between the terminal cyano and MeOH ligands of neighbouring cluster molecules. For the latter, the isotropic interaction energy between two magnetic dipoles of S = $^{51}/_2$ separated by 17.5 Å, *i.e.* the distance between the cen-

tres of nearest neighbour clusters, is in the order of 0.2 cm^{-1}. The estimate of 0.2 cm^{-1} is valid at the very lowest temperatures with only the $S = {}^{51}/_{2}$ cluster level populated. Around 40 K it is definitely lower because of the population of cluster levels with lower S values. From a calculation on the cluster fragments in Fig. 4, a mean spin value of about $S = 12$ can be extrapolated for the whole cluster at T = 40 K. This S value results in a magnetic dipolar interaction energy in the order of 0.05 cm^{-1}. Using these values and the molecular-field approximation, we estimate a T_c of about 30 K. This is in reasonably good agreement with the observed onset of cooperative intercluster correlations around 40 K. We conclude that magnetic dipolar interactions account for the major part of intercluster correlations in this temperature range. Magnetisation data collected at several temperatures between 2 K and 60 K with applied fields of up to 50 kG are shown in Fig. 6. The curve at 2K exhibits a very high zero-field susceptibility and reaches a saturation value near the expected $M_S/N\beta$ value of 51 for an $S = {}^{51}/_{2}$ ground state calculated with a value of g(cluster) = 2.0.

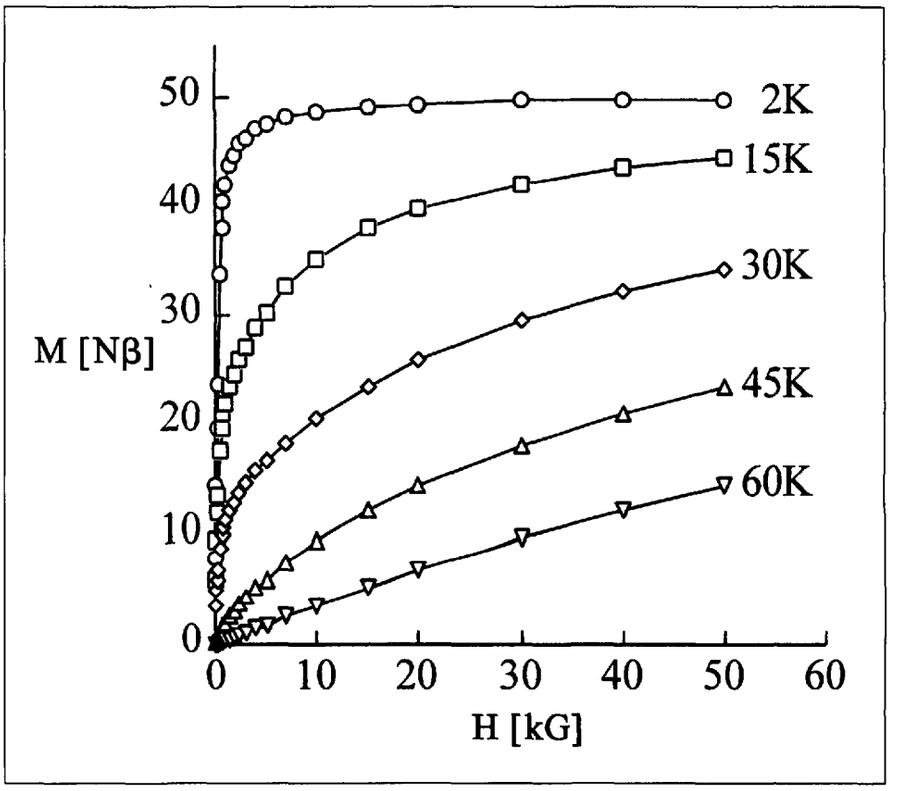

Fig. 6. Field dependence of the magnetisation M for the polycrystalline cluster compound **1** at different temperatures.

In contrast to other high-spin clusters, such as Mn_{12}-acetate [16], this compound does not exhibit the typical phenomena of molecular hysteresis and slow quantum tunnelling at low temperatures. We conclude that in the low temperature regime, below 50 K, where magnetic ordering seems to arrive, we have a competitive interplay of intra- and intercluster interactions and modelling of this magnetic data is not yet possible because this new and interesting situation has not been dealt with theoretically to-date. From these observations however, it now becomes apparent that dipole-dipole intercluster interactions will become increasingly important with increasing ground state S values of high-spin clusters; it will therefore be increasingly difficult to observe typical nano-magnetic properties of spin clusters, unless specific measures are taken to isolate or insulate them.

4.3. *New Related Molecular Clusters*

Working towards the isolation of single cluster magnetic characteristics at low temperature, we have succeeded in preparing the ethanol analogue of compound **1**, a cluster of stoichiometry $[Mn^{II}\{Mn^{II}(EtOH)_3\}_8(\mu\text{-}CN)_{30}\{Mo^{V}(CN)_3\}_6]\cdot 6EtOH\cdot MeOH$ (**2**) [18], where larger ethanol molecules now complete the coordination sphere of the peripheral Mn^{II} ions. The molecular geometry of **2** has been determined by low temperature single crystal X-ray crystallography [18]. The compound once again consists of cyanide-bridged $Mn^{II}_9Mo^{V}_6$ units, with nine Mn^{II} ions defining a body-centred cube and six Mo^{V} ions constituting an octahedron. In contrast to **1**, the molecule crystallises in the triclinic space group ($P\bar{1}$), with a central Mn^{II} ion occupying each corner of the unit cell. Structurally, a slight change in the packing motif has been observed which better accommodates the bulkier ethanol molecules, each cluster being surrounded by six instead of eight nearest neighbours. This in turn has had a subtle effect on the closest intercluster metal-metal contacts which are in the range 6.82–7.18 Å for $Mo^{V}\cdots Mn^{II}$, and 7.36-8.23 Å for $Mn^{II}\cdots Mn^{II}$. Compared to cluster **1**, the $Mo^{V}\cdots Mn^{II}$ contacts are on average 0.4 Å shorter, whereas the $Mn^{II}\cdots Mn^{II}$ interactions are 0.4 Å longer. The cluster to cluster distance is found to be shorter for this cluster namely, 17.2 Å compared to 17.5 Å for cluster **1**.

The intermolecular network of H-bonding interactions has remained essentially intact; the ethanol ligands on neighbouring clusters are simply not bulky enough to disturb these inter-cluster interactions. They are in fact, able to well-accommodate these interactions by twisting away from each other, thus minimising steric interactions and enabling neighbouring clusters to pack close together (Fig. 7). The shortest O–H···N contacts between adjacent clusters (2.74 Å) are exactly within the range of the H-bonding interactions previously reported for cluster **1**. Once again, each peripheral Mn^{II} ion in a cluster has one ethanol ligand which is involved in an intermolecular bond to the nitrogen of a cyano ligand in a neighbouring cluster. All remaining terminal cyano and ethanol ligands are hydrogen bonded to solvent molecules. Cluster **2** has very similar magnetic properties to those already described for **1**. The T_c for this compound has been estimated to be approximately 34 K, which is slightly lower than the ordering temperature of 44 K reported for cluster **1**.

These molecules provide us with a new class of materials for study in the field of molecular magnetism. Detailed investigations into the large variety of chemical clusters with analogous stoichiometries are currently ongoing in our laboratory. Our aim is to control the spin multiplicity and hence tune the magnetic properties by varying the metal ions. We have had success in preparing the

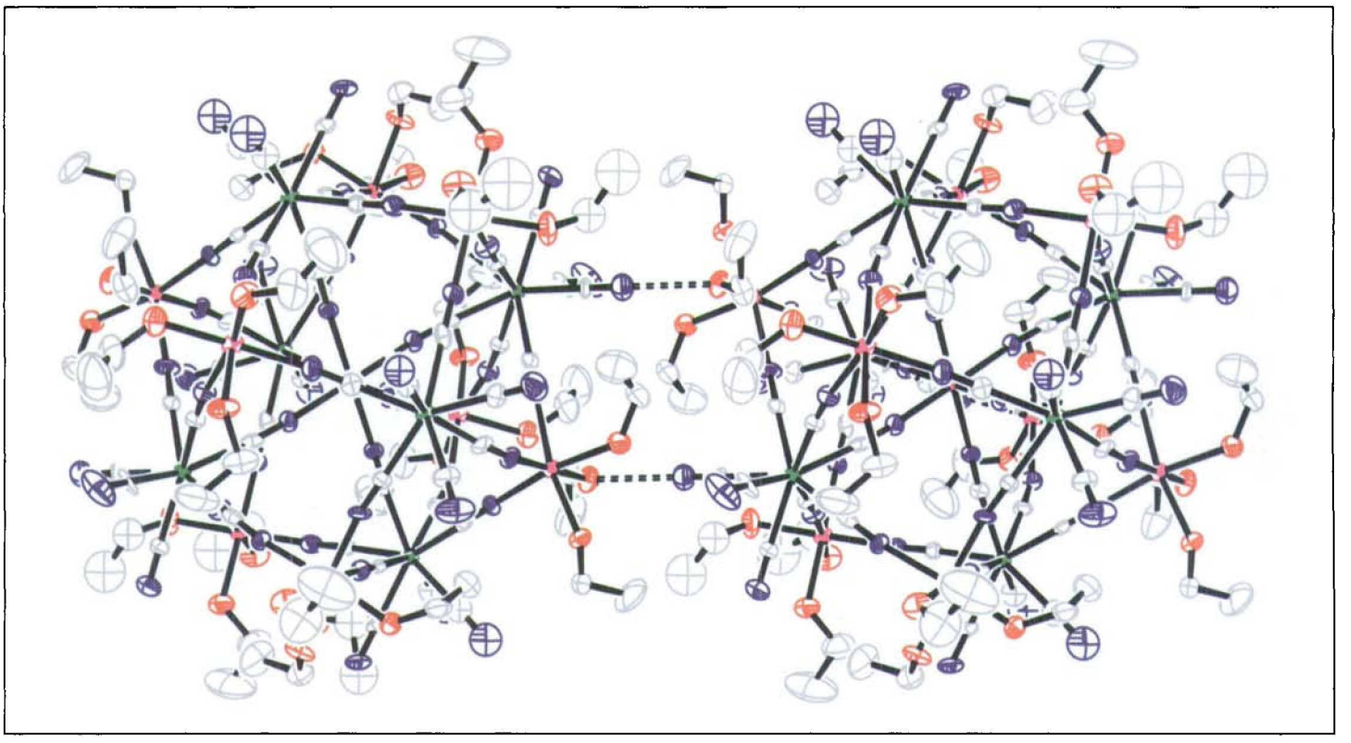

Fig. 7. ORTEP representation of two nearest neighbour clusters (**2**) with ethanol ligands on the outer Mn^{II} ions. H-atoms are omitted for clarity. Dotted lines represent the shortest O–H···N contacts (2.74 Å) between adjacent clusters.

cyanide-bridged $Co^{II}{}_9Mo^{V}{}_6$ molecular cluster whose structure has been confirmed by single crystal X-ray crystallography [19]. This compound is isostructural with cluster **1** and a detailed investigation into the magnetic properties is currently in progress. Apart from varying the M^{II} ions we are also varying the octacyanometalate $[BCN_8]^{3-}$ precursor. We have very recently prepared the cyanide-bridged $Co^{II}{}_9W^{V}{}_6$ molecular cluster whose structure is confirmed by single crystal X-ray crystallography [20]. The magnetic properties of this molecule are also currently under investigation. In parallel studies, the group of Hashimoto has also had recent success in preparing a high-spin cyanide-bridged $Mn^{II}{}_9W^{V}{}_6$ molecular cluster [21]. This compound has been characterised both structurally and magnetically. Interestingly, in contrast to our clusters, the molecule crystallises in the higher symmetry, trigonal space group ($R\bar{3}$), which imposes a three-fold axis on the cluster passing through the central Mn^{II} ions. The stoichiometry is very similar to **2** in the respect that the outer ligands on the peripheral Mn^{II} ions are ethanol molecules. The distance between centres of nearest neighbour clusters is 17.5 Å which is identical to that found for cluster **1**, but slightly longer (0.3 Å) than that found for cluster **2**. The shortest inter-cluster contact between metal ions is 7.1 Å, which is comparable with 6.8 Å and 7.0 Å for Mn···Mo contacts in clusters **1** and **2**, respectively. The magnetic data for this cluster in the low temperature regime supports an $S = {}^{39}/_{2}$ ground state spin which corresponds to an antiferromagnetic coupling of the spins on the Mn^{II} and the W^{V} ions through the cyanide bridges. This cluster does not display bulk magnetic behaviour at low temperatures, presumably, the ground state spin value is not large enough for intermolecular dipole-dipole interactions to take effect. In summary, by varying the $[BCN_8]^{3-}$ building blocks together with the M^{2+} ions we can retain the overall cluster topology, but the crystallographic symmetry imposed on the cluster is an important consideration, since it may have a significant influence on the ordering of the spins on the metal ions. Bearing these factors in mind, we are now able to design and control spin multiplicity in the molecular clusters by selecting the constituent metal ions.

5. Extended Three-Dimensional Networks

In work parallel to the above, we have investigated the effects of changing the oxidation state of the metal in the cyanometalates building block moving from B^{V} to B^{IV}, (B = Nb, Mo, W). This work was motivated by the idea that these compounds could be structurally and magnetically very different from the molecular clusters described above. Reaction of the octacoordinated $[BCN_8]^{4-}$ precursor together with various M^{II} ions has, as anticipated, prevented us from obtaining molecular clusters and yielded a second class of interesting μ-cyano-bridged compounds with novel structural and physical properties.

5.1. *Structural Topology*

Reaction of $[Nb^{IV}CN_8]^{4-}$ with a Mn^{II} salt afforded a red crystalline compound which was shown by single crystal X-ray analysis to be a cyano-bridged extended three-dimensional network of stoichiometry $[Nb^{IV}\{(\mu\text{-}CN)_4Mn^{II}(H_2O)_2\}_2]$, (**3**) [11]. The network comprises of Nb^{IV} ions which are connected to nearest neighbour Mn^{II} ions through cyanide bridges in a three-dimensional arrangement. The compound crystallises in the tetragonal space group *I*4/m, with one Nb^{IV} metal ion sitting on the crystallographic four-fold rotation axis and a Mn^{II}, together with two co-ordinating water molecules occupying a crystallographic mirror plane. Each Nb^{IV} ion is

connected through eight μ-cyano-ligands to neighbouring Mn^{II} ions. The environment around the Nb^{IV} atom is closest to square antiprismatic, in contrast to that of the Mo^{V} ion in the cluster which is closer to a dodecahedral geometry. The Nb-C-N bond angles deviate slightly from 180° and are in the range 175.3° to 175.9°. The Mn^{II} ions are in an octahedral environment, bonded to four Nb^{IV} ions through cyanide bridges; two axial water molecules complete the six-fold coordination. The three-dimensional organisation can be best described as a grid-like arrangement of [Mn-NC-Nb-CN] motifs running along the *c* direction of the unit cell (Fig. 8). Each Nb^{IV} metal ion is connected through cyano bridges to four Mn^{II} ions of the type (Mn(1A) Mn(1C) directly above and four Mn^{II} ions of the type Mn(1) and Mn(1B) directly below, and in this way a three-dimensional grid is built up, (Fig. 9).

The distance between adjacent neighbouring Nb^{IV} ions in a single motif is 6.64 Å for Nb(1)···Nb(1A) and the shortest distance between two Mn^{II} ions is 6.12 Å for Mn(1)···Mn(1C) and Mn(1)···Mn(1B). The Mn^{II} ions are situated either above or below the planes containing the Nb^{IV} ions and the shortest metal–metal contacts are 5.45 Å, between Nb^{IV}···Mn^{II} metal ions of adjacent layers. Axial-coordinated water molecules point directly into the channels of the network and are involved in H-bonding interactions, the shortest contact being 2.69 Å, for axial Mn–O–H···O–Mn interactions. A view directly down the four-fold axis shows clearly the channels in the network containing coordinated as well as free solvent waters (Fig. 10). Intermolecular contacts involving the solvent molecules are all larger than the sum of the van der Waals radii, the shortest being 2.98 Å between two solvent waters.

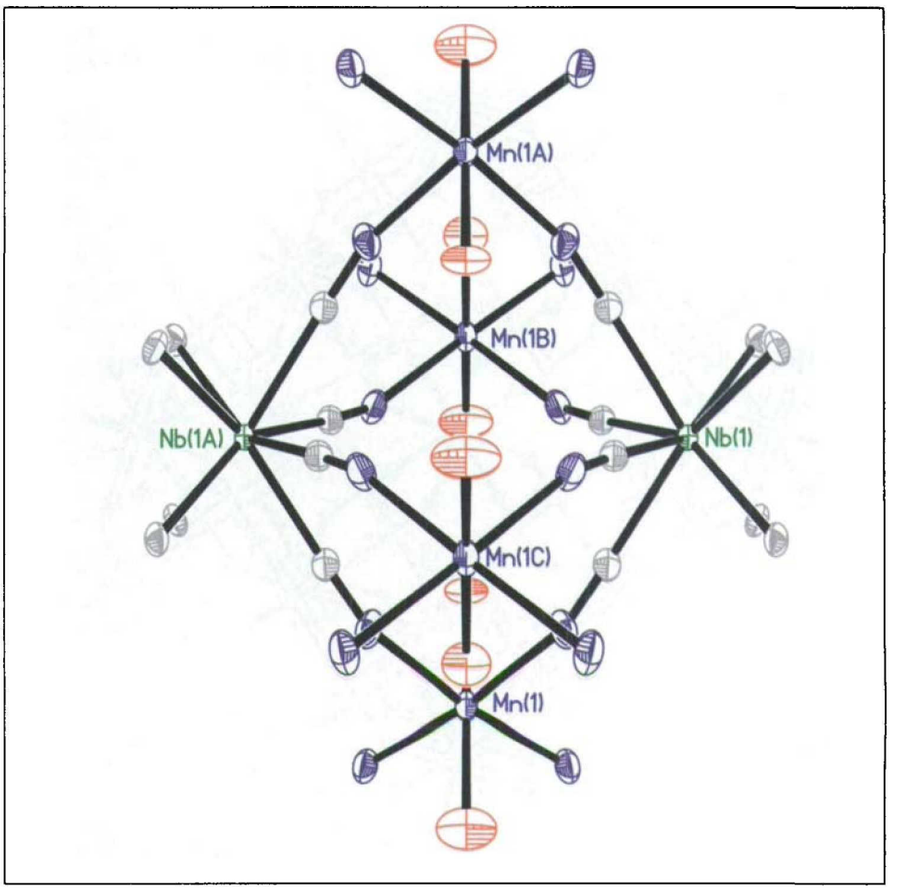

Fig. 8. ORTEP representation focusing on a repeating motif (**3**).

5.2. *Magnetic Properties*

The magnetic susceptibility of a polycrystalline sample of compound **3** has been measured in the temperature range from 300 to 1.8 K. The plot of χ_M *vs.* T is shown in Fig. 11.

Most significantly, the χ_M curve exhibits a clear break around 50 K where χ_M starts to rise steeply to a value of 3000 emu K mol^{-1} in the product χ_M·T per stoichiometric unit and for an applied field of 50 G. This abrupt increase of χ_M indicates the onset of cooperative ferromagnetic interactions.

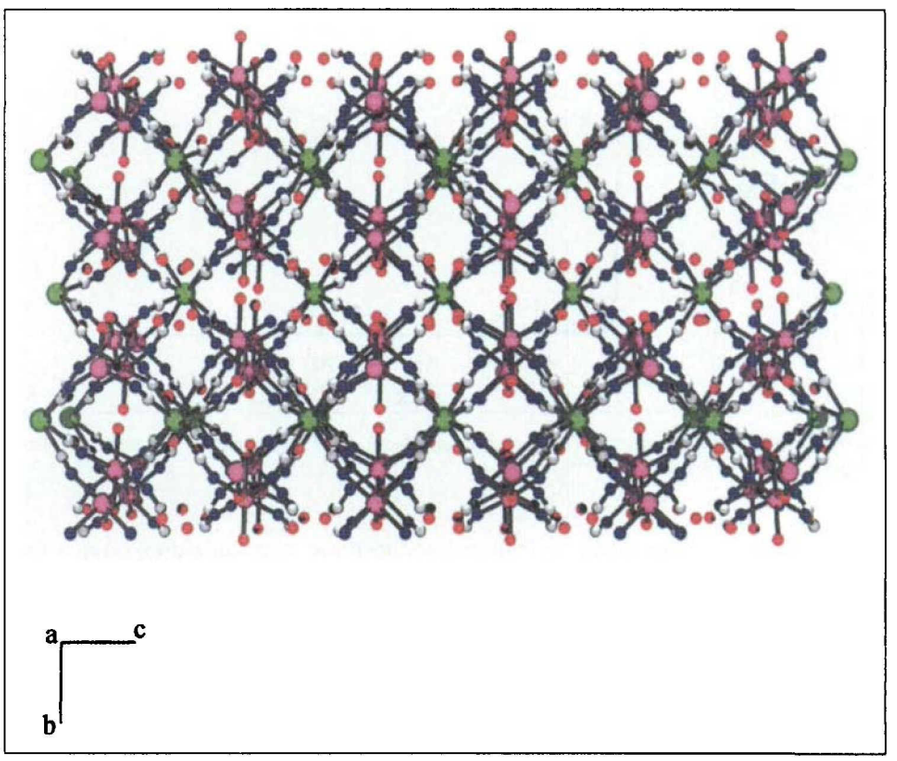

Fig. 9. Structure of compound **3** showing the grid-like arrangement of repeating [Mn-NC-Nb-CN] running along the *c*-axis of the unit cell.

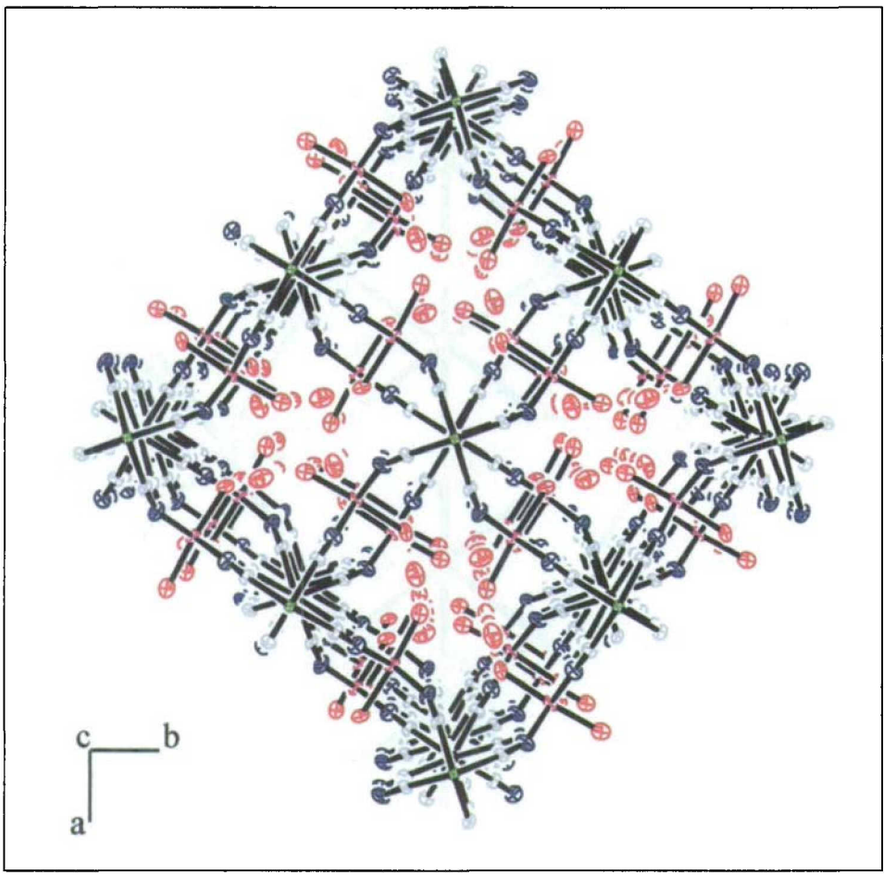

Fig. 10. ORTEP representation of compound **3** viewed down the crystallographic four-fold axis.

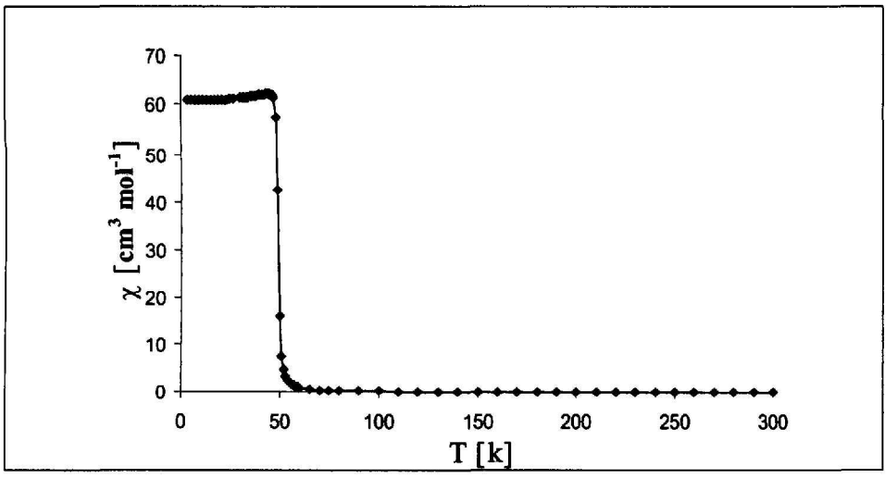

Fig. 11. Temperature dependence of χ_M for an applied field of 50 Gauss for the polycrystalline compound **3**.

To confirm the characteristic behaviour of the ferromagnetically correlated phase, the temperature dependencies of the magnetisation M under a weak magnetic field (1 G) and the remanent magnetisation were measured. The field-cooled magnetisation (FCM), zero-field-cooled magnetisation (ZFCM) and remanent magnetisation (RM) curves are shown in Fig. 12 and altogether, they can be attributed to a three-dimensional ferromagnetic phase transition at 50 K.

Finally, the magnetisation data collected at 2 K with applied fields of up to 10 kG are shown in Fig. 13. The magnetisation *versus* field curve exhibits a high zero-field susceptibility and reaches a saturation value near 9.5 Nβ. Obviously, this value is too low to account for a fully parallel alignment of all the free spins which suggests the occurrence of a canting angle between neighbouring spins. In order to elucidate in detail the specific magnetic structure of the compound, an elastic neutron-scattering experiment has been started on a deuterated compound of **3** at the SINQ facilities of the PSI in Villigen. Thereby, the occurrence of distinct magnetic neutron peaks has already been established and the exact data analysis is still in progress.

We have recently prepared $Fe^{II}W^{IV}$ as well as $Fe^{II}Mo^{IV}$ and $Mn^{II}Mo^{IV}$ analogues, whose structures have been shown by single crystal X-ray diffraction [22] to be three-dimensional networks, isostructural with that of compound **3**.

6. Summary

This work demonstrates the versatility of octacyanometalate building blocks for the self-assembly of two new classes of compounds namely, molecular clusters and extended three-dimensional networks. We can conclude that within the first class of compounds, namely the molecular clusters, it is clearly possible to observe both ferromagnetic and antiferromagnetic interactions between metal ions through the μ-cyanide linkages, and that the number of unpaired spins clearly dictates if the molecule has purely single-molecule characteristics or single-molecule characteristics interwoven with bulk properties. By varying the oxidation state of the octacyanometalate building block we can completely alter the molecular structure and prepare a second class of compounds that display bulk ferromagnetic properties. Hence by tuning the metal ions, we can move from single-molecular magnets to bulk ferromagnets with relatively little synthetic effort. This work demonstrates the usefulness and versatility of cyanometalate building blocks for applications in the field of molecule-based magnets. Ongoing studies focus on the elucidation of the magnetic structures of these compounds, as well as detailed structural studies to develop a straightforward concept for the synthesis of new materials from cyanometalate building blocks, having a predictable structural order and a useful set of solid-state properties.

Received: August 16, 2000

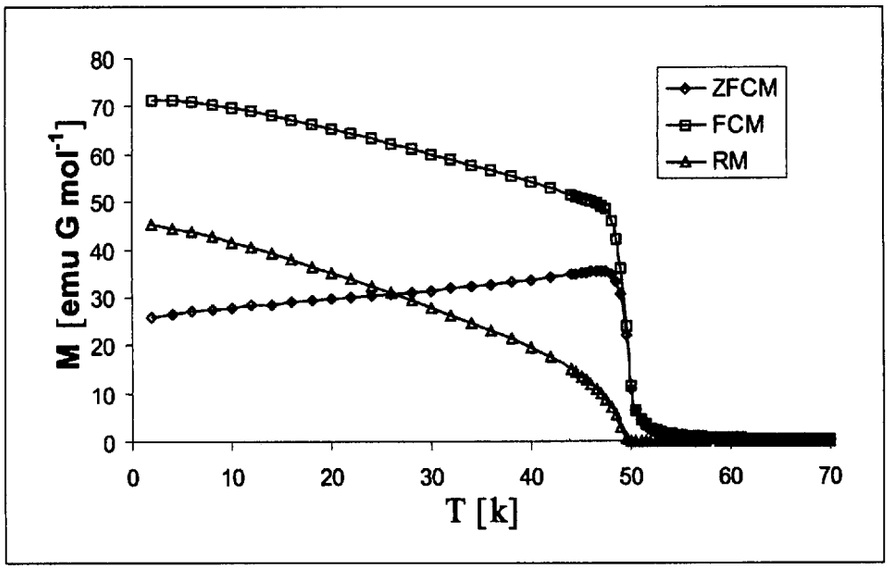

Fig. 12. Temperature dependence of the magnetisation M, measured on a polycrystalline sample of **3**, by ZFCM, FCM, as well as the remanent magnetisation.

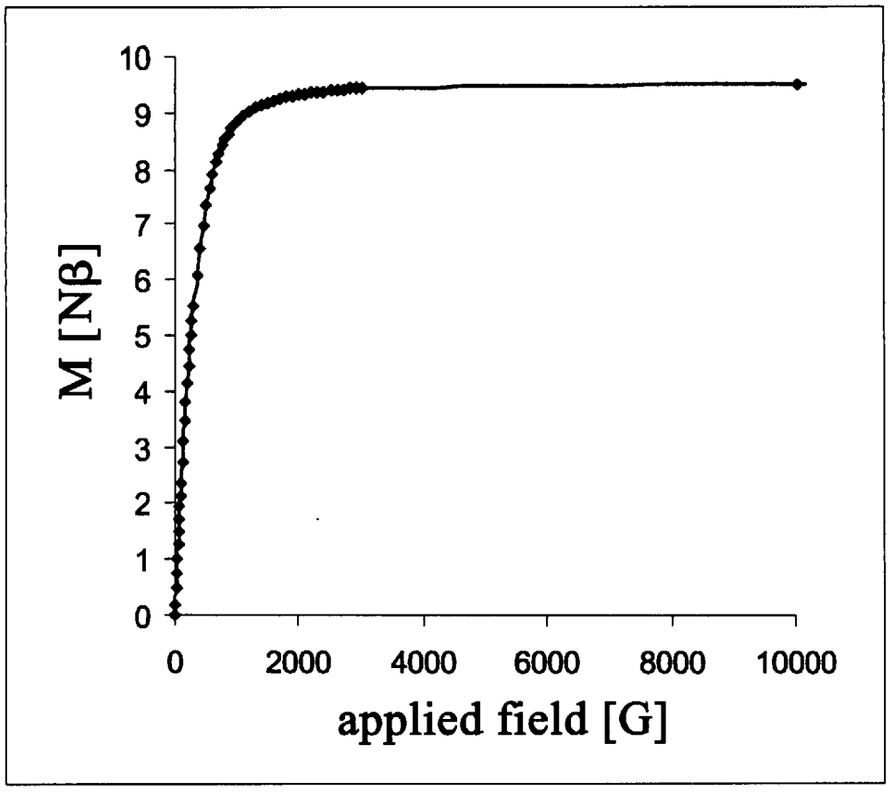

Fig. 13. Field dependence of the magnetisation M, measured at 2 K on a polycrystalline sample of **3**.

[1] O. Kahn, 'Molecular Magnetism', Wiley-VCH, Weinheim, **1993**.
[2] J-M. Lehn, 'Supramolecular Chemistry, Concepts and Perspectives', Wiley-VCH, Weinheim, **1995**.
[3] O. Kahn, *Chemistry in Britain*, February **1999**, 24–27.
[4] M. Pilkington, S. Decurtins, in 'Magnetoscience – From Molecules to Materials', Eds. J.S. Miller, M. Drillon, Wiley-VCH, Weinheim, **2000**, in print.
[5] S. Decurtins, *Chimia* **1998**, *52*, 539–546.
[6] Misc. Berolinesia and Incrementum Sci. *1* Berlin, **1710**, 337.
[7] A. Werner, *Zeitschr. Anorg. Chem.* **1893**, *3*, 267.
[8] S. Ferley, T. Mallah, R. Ouahès, P. Veillet, M. Verdaguer, *Nature (London)* **1995**, *378*, 701–703.
[9] O. Kahn, *Nature (London)* **1995**, *378*, 667–668.
[10] J. Larionova, M. Gross, M. Pilkington, H-P. Andres, H. Stoeckli-Evans, H.U. Güdel, S. Decurtins, *Angew. Chem. Int. Ed.* **2000**, *39*, 1605–1609.
[11] M. Pilkington, P. Franz, S. Decurtins, M. Verdaguer, *Inorg. Chem.* **2000**, submitted for publication.
[12] S.M.J. Aubin, M.W. Wemple, D.M. Adams, H.L. Tsai, G. Christou, D. Hendrickson, *J. Am. Chem. Soc.* **1996**, *118*, 7746–7754.
[13] G. Aromi, M. J. Knapp, J-P. Claude, J.C. Huffman, D.N. Hendrickson and G. Christou, *J. Am. Chem. Soc.* **1999**, *121*, 5489–5499.
[14] A.L. Barra, A. Caneschi, A. Cornia, F. Fabrizi de Biani, D. Gatteschi, C. Sangreggario, R. Sessoli and L. Sorace, *J. Am. Chem. Soc.* **1999**, *121*, 5302–5310.
[15] L. Thomas, F. Lionti, R. Ballou, D. Gatteschi, R. Sessoli, B. Barbara, *Nature* **1996**, *383*, 145–147 and all references herein.
[16] A. Caneschi, D. Gatteschi, R. Sessoli, A.L. Barra, L.C. Brunel, M. Guillot, *J. Am. Chem. Soc.* **1991**, *113*, 5873–5874.
[17] D. Altbir, P. Vargas, J. d'Albuquerque e Castro, U. Raff, *Phys. Rev. B* **1998**, *57*, 13604–13609.
[18] M. Pilkington, M. Gross, L. Gilby, S. Decurtins, **2000**, manuscript in preparation.
[19] M. Pilkington, J. Larionova, M. Gross, S. Decurtins, **2000**, unpublished results.
[20] F. Bonadio, S. Decurtins, H. Stoeckli-Evans, **2000**, unpublished results.
[21] Z.J. Zhong, H. Seino, Y. Mizobe, M. Hidai, A. Fujishima, S. Ohkoshi, K. Hashimoto, *J. Am. Chem. Soc.* **2000**, *122*, 2952–2953.
[22] M.Pilkington, M. Biner, S. Decurtins, H. Stoeckli-Evans, unpublished results.